DOI:
10.1039/C6DT03811E

Document Version
Peer reviewed version

Journal Name

ARTICLE

The Breast Cancer Stem Cell Potency of Copper(II) Complexes Bearing Nonsteroidal Anti-Inflammatory Drugs and Their Encapsulation Using Polymeric Nanoparticles

Received 00th January 20xx,
Accepted 00th January 20xx

DOI: 10.1039/x0xx00000x

www.rsc.org/

Arvin Eskandari,[a] Janine N. Boodram,[a] Paul B. Cressey,[a] Chunxin Lu,[a] Peter M. Bruno,[b] Michael T. Hemann,[b] and Kogularamanan Suntharalingam[a]*

We report the cancer stem cell (CSC) potency of a novel series of copper(II)-phenanthroline complexes bearing nonsteriodial anti-inflammotory drugs; naproxen, tolfenamic acid, and indomethacin (**2a**-**3c**). Two of the complexes, **2a** and **3c**, kill breast CSC-enriched HMLER-shEcad cells (grown in both monolayer and three-dimensional cell cultures) to a significantly better extent than salinomycin, a well-established CSC toxin. The most potent complex in the series, **3c** induces its cytotoxic effect by generating intracellular reactive oxygen species (ROS) and inhibiting cyclooxgenase-2 (COX-2) activity. Encapsulation of **3c** using biodegradable methoxy poly(ethylene glycol)-b-poly(D,L-lactic-co-glycolic) acid (PEG-PLGA) copolymers at the appropriate feed (5%, **3c NP^5**) enhances breast CSC uptake and reduces overall toxicity. The nanoparticle formulation, **3c NP^5** selectively kills breast CSCs over bulk breast cancer cells, and evokes a similar cellular response to the payload, **3c**. To the best of our knowledge, this is the first study to demonstrate that polymeric nanoparticles can be used to effectively deliver CSC-potent metal complexes into CSCs.

Introduction

Cancer stem cells (CSCs) are a distinct population of tumour cells that have the ability to self-renew, differentiate, and form metastatic tumours.[1] CSCs effectively evade conventional chemotherapy and radiotherapy as these treatments specifically target fast growing cancer cells, and CSCs, due to their stem cell-like properties, divide more slowly.[2] After surviving treatment, CSCs are able to regenerate the original tumour and/or produce invasive cancer cells that are able to colonise distant organs.[3] For these reasons, CSCs are widely thought to be responsible for cancer relapse.[4] Therefore, to provide a durable response and prevent tumour recurrence, chemotherapeutics must have the ability to remove the entire population of cancer cells, including CSCs. Therapeutic strategies capable of selectively killing CSCs and disrupting the microenvironments (niches) supporting these cells are the focus of several research programmes.[5,6] Potential CSC therapeutic targets such as cell surface markers[7-11] and various deregulated signalling pathways[12-14] have been identified, but there is still no clinically approved drug that specifically kills CSCs. Most of the compounds undergoing pre-clinical or clinical investigation as CSC-specific agents are completely organic in nature.[2] The anti-CSC properties of metal-containing compounds are largely unexplored.[15-17]

We recently reported a series of copper(II)-phenanthroline complexes containing the nonsteroidal anti-inflammatory drug (NSAID), indomethacin, capable of selectivity killing breast CSCs over bulk breast cancer cells.[18] The most effective compound in this series, **1** (see Fig. 1) induced breast CSC toxicity by generating intracellular reactive oxygen species (ROS) and inhibiting cyclooxygenase-2 (COX-2), an enzyme that catalyses prostaglandins (PG) formation and involved in inflammatory response. The breast CSC selectivity of **1** is thought to arise from its ability to exploit the vulnerability of breast CSCs to changes in their intracellular redox state,[19,20] and the differential expression of COX-2 in breast CSCs and bulk breast cancer cells.[18,21,22] Here, we have sought to increase the CSC potency of the copper(II)-phenanthroline series by, (i) increasing their inherent lipophilicity (to improve

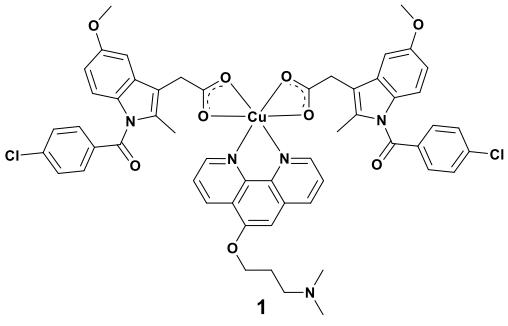

1

Fig. 1 Chemical structure of a copper(II)-phenanthroline complex bearing two indomethacin molecules, which was previously reported to selectively kill breast CSCs over bulk breast cancer cells.

[a] *Department of Chemistry, King's College London, London, SE1 1DB, United Kingdom. E-mail: kogularamanan.suntharalingam@kcl.ac.uk*
[b] *The Koch Institute for Integrative Cancer Research, Massachusetts Institute of Technology, Massachusetts, 02139, United States*

Electronic Supplementary Information (ESI) available: [details of any supplementary information available should be included here]. See DOI: 10.1039/x0xx00000x

cell uptake and nanoparticle encapsulation, *vide infra*), and (ii) varying the NSAID component. Specifically, 3,4,7,8-tetramethyl-1,10-phenanthroline and 4,7-diphenyl-1,10-phenanthroline were used to increase hydrophobicity, while naproxen, tolfenamic acid, and indomethacin were used to modulate COX-2 activity.

Nanoparticles offer a method to unambiguously deliver chemotherapeutics to tumours (including CSCs).[23] Further, nanosystems increase drug solubility, bioavailability, drug half-life, and reduce off-target toxicity.[24,25] Spherical nanoparticles with diameters ranging from 100-200 nm can passively target cancer cells by taking advantage of the enhanced permeability and retention (EPR) effect in tumour tissues.[26,27] Several spherical nanoparticle formulations exist, including those based on iron-oxide, gold, liposomes, and polymers.[28] A number of these formulations are currently used in the clinic to deliver chemotherapies to tumours.[29] Nanoparticles comprising of polymers are of particular interest due to their synthetic versatility and tuneable properties.[30] Polymeric nanoparticles have been widely used to deliver metallodrugs to cancer cells in vitro and in vivo,[31-34] however, their ability to transport CSC-potent metal complexes into CSCs has not been investigated. It should be noted that nanoparticle platforms for CSC-targeted drug delivery of non-metal based therapeutics have been reported.[35-38] In the present, proof-of-concept study, we use the biodegradable, amphiphilic copolymer, methoxy poly(ethylene glycol)-*b*-poly(D,L-lactic-co-glycolic) acid (PEG-PLGA), to encapsulate and deliver the most CSC-potent and -selective copper(II) complex in the reported series, **3c**, into breast CSCs.

Results and discussion

Synthesis and characterisation

The copper(II) complexes investigated in this study are depicted in Fig. 2. The copper(II)-NSAID complexes, **2a**-**3c** were prepared by reacting $CuCl_2 \bullet 2H_2O$ with 3,4,7,8-tetramethyl-1,10-phenanthroline or 4,7-diphenyl-1,10-phenanthroline and two equivalents of the appropriate NSAID ligand (naproxen, tolfenamic acid, or indomethacin) in methanol, under basic conditions. The copper(II) complexes were isolated as green or blue solids and were fully characterised by mass spectrometry, infra-red spectroscopy, and elemental analyses (full details reported in the Supporting Information).

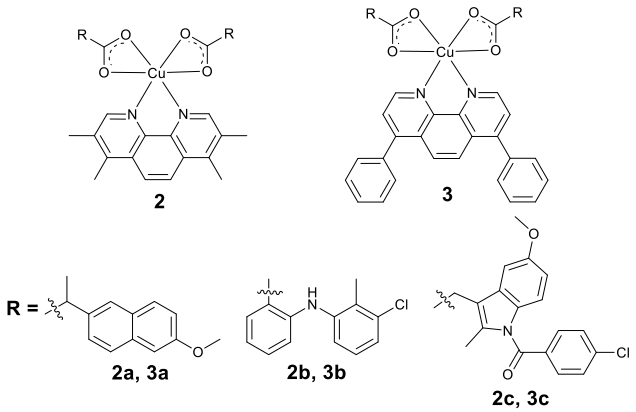

Fig. 2 Structures of the copper(II)-phenanthroline complexes bearing NSAIDs (naproxen, tolfenamic acid, or indomethacin) that are under investigation.

The lipophilicity of the copper(II)-NSAID complexes, **2a**-**3c** was determined by measuring the extent to which they partitioned between octanol and water, P. The experimentally determined Log P values for **2a**-**3c** varied between 0.89 and 1.01 (Table S1). The hydrophobic nature of the complexes suggests that **2a**-**3c** will be readily absorbed by cells. UV-Vis spectroscopy studies were performed to evaluate the stability of **3c**, taken as a representative member of the copper(II)-NSAID series, in biologically relevant solutions. In PBS containing whole cell lysate (5 x 10^3 HMLER-Ecad cells), **3c** (50 μM) is reasonably stable over a period of 24 h at 37 °C (Fig. S1). In the presence of ascorbic acid (500 μM in PBS, 10 equivalence), a cellular reductant, the absorption of **3c** markedly decreased over 24 h (Fig. S2). The lower stability of **3c** in the presence of ascorbic acid is most likely a result of reduction of the metal centre from copper(II) to copper(I). Before carrying out cellular studies, the stability of **3c** in mammary epithelial cell growth medium (MEGM) was investigated at 37 °C (Fig. S3). Under these conditions, **3c** is adequately stable over the course of 24 h.

Potency towards breast CSC-enriched and CSC-depleted cells

In order to determine the breast CSC potency and selectivity (over bulk breast cancer cells) of **2a**-**3c**, two human mammary epithelial cell lines were used; HMLER and HMLER-shEcad cells. HMLER cells express a stable CSC-like population of 5−8%, whereas HMLER-shEcad cells exhibit a 90% CSC-like population.[39] The cytotoxicity of **2a**-**3c** towards HMLER and HMLER-shEcad cells was measured using the MTT [3-(4,5-dimethylthiazol-2-yl)-2,5-diphenyltetrazolium bromide] assay. IC_{50} values (concentrations required to induce 50% viability) were determined from dose-response curves (Fig. S4-5) and are summarised in Table 1 and S2. Salinomycin, a natural

Table 1. IC_{50} values of the copper(II) - nonsteroidal anti-Inflammatory drug complexes, **1-3c**, cisplatin, dichloro(1,10-phenanthroline)copper(II), and salinomycin against HMLER and HMLER-shEcad cells.

Compound	HMLER IC_{50} [μM] [a]	HMLER-shEcad IC_{50} [μM] [a]
1 [b]	7.38 ± 0.30	2.21 ± 0.46
2a	0.54 ± 0.27	0.28 ± 0.03
2b	4.71 ± 1.08	2.42 ± 0.12
2c	0.59 ± 0.25	0.79 ± 0.06
3a	0.27 ± 0.09	0.25 ± 0.04
3b	0.88 ± 0.30	2.65 ± 0.04
3c	0.46 ± 0.16	0.23 ± 0.04
cisplatin	3.44 ± 0.47	4.85 ± 0.36
dichloro(1,10-phenanthroline)copper(II) [b]	4.90 ± 0.17	7.86 ± 0.26
salinomycin	16.43 ± 2.09	5.63 ± 0.11

[a]Determined after 72 h incubation (mean of three independent experiments ± SD). [b] Reported in reference 18.

product that was previously shown to specifically inhibit breast CSC proliferation, was used as a positive control (Fig. S6).[39] Cisplatin and dichloro(1,10-phenanthroline)copper(II) (chosen as a representative copper(II) complex without a NSAID moiety) were included as additional controls (Fig. S7). The copper(II)-NSAID complexes, **2a**-**3c** displayed micromolar or sub-micromolar potency towards both cell lines. Two of the complexes, **2b** and **3c** displayed significantly greater potency ($p < 0.05$) for CSC-enriched HMLER-shEcad cells than CSC-deficient HMLER cells. The naproxen and indomethacin bearing complexes, **2a** and **3c** exhibited greater potency toward HMLER-shEcad cells than salinomycin (up to 24-fold), cisplatin (up to 21-fold), and dichloro(1,10-phenanthroline)copper(II) (up to 34-fold). However it should be noted that salinomycin is 3-fold more cytotoxic towards HMLER-shEcad cells than HMLER cells, whereas the copper(II) complexes are, at most, only 2-fold more selective. Notably, the copper(II) complexes, **2a** and **3c** exhibited 10-fold higher potency for HMLER-shEcad cells than **1** (IC_{50} = 2.2 μM), the lead compound from our previous study.[18] Naproxen was non-toxic towards both cell lines (> 100 μM) whereas tolfenamic acid displayed moderate activity (Fig. S8-9). This is consistent with the low cytotoxicity previously observed for indomethacin.[18]

Cellular uptake by breast CSC-enriched HMLER-shEcad cells

Cellular uptake studies were conducted to determine the CSC permeability of the copper(II) complexes, **2a**-**3c**. HMLER-shEcad cells were incubated with **2a**-**3c** (at their respective IC_{50} values for 12 h) and the intracellular copper concentration was determined by inductively coupled plasma mass spectrometry (ICP-MS). The copper(II) complexes, **2a**-**3c** were readily taken up by HMLER-shEcad cells, with whole cell uptake ranging from 56.0 ± 0.5 ppb of Cu/ million cells for **2a** to 120.9 ± 1.0 ppb of Cu/ million cells for **2c** (Fig. 3). A modest correlation between cell uptake and the NSAID or phenanthroline component was observed. Complexes containing indomethacin (**2c** and **3c**) were internalised better than those bearing tolfenamic acid (**2b** and **3b**) or naproxen (**2a** and **3a**). Complexes possessing 4,7-diphenyl-1,10-phenanthroline (**3b** and **3c**) were taken up marginally better than those containing 3,4,7,8-tetramethyl-1,10-phenanthroline (**2b** and **2c**). The relatively small variation in cell uptake across the copper(II) complexes (64.9 ppb of Cu/ million cells) is consistent with their similar lipophilicities (Log P values, Table S1). The indomethacin-appended complexes, **2c** and **3c** exhibited greater cell penetration (up to 2.2-fold) than **1** (which also contains indomethacin) under identical conditions. This was expected as the 3,4,7,8-tetramethyl-1,10-phenanthroline and 4,7-diphenyl-1,10-phenanthroline ligands present in **2c** and **3c** are more hydrophobic, and thus more susceptible to passive uptake, than the amine substituted phenanthroline ligand found in **1**. A direct correlation between cellular uptake and cytotoxicity was not observed for **2a**-**3c**.

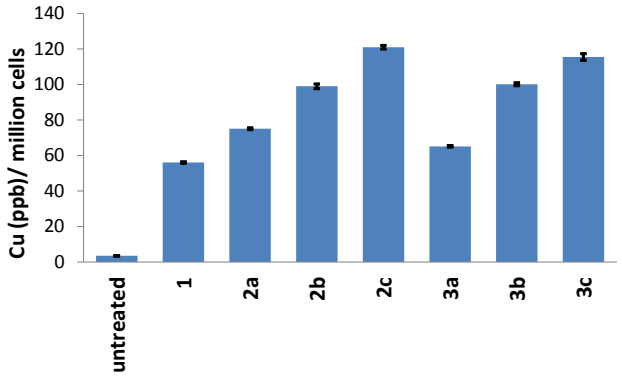

Fig. 3 Copper content in HMLER-shEcad cells untreated and treated with **2a**-**3c** and **1** (at their respective IC50 values for 12 h).

Mammosphere potency

Breast CSCs when grown in serum-free media, under low-attachment conditions are capable of forming three-dimensional, tumour-like structures called mammospheres.[40] The ability of a given compound to inhibit mammosphere formation from single cell suspensions (with respect to number and size) is often used as a marker for CSC potency. The ability of **2a**, **2b**, and **3c** to inhibit HMLER-shEcad mammosphere formation (at their respective IC_{20} values after 5 days incubation) was assessed using an inverted microscope. Incubation with **2a**, **2b**, and **3c** markedly reduced the number and size of mammospheres formed (Fig. 4 and S10). Incubation with cisplatin (at the IC_{20} value after 5 days incubation) also reduced the size of mammospheres formed but to a lesser extent than **2a**, **2b**, and **3** (Fig. 4). Treatment with free NSAIDs; naproxen, tolfenamic acid, or indomethacin did not significantly affect the number of mammospheres formed (Fig. S10). In order to determine the ability of **2a**, **2b**, and **3c** to reduce mammosphere viability, TOX8, a resazurin-based reagent, was used. The IC_{50} values (concentration required to reduce mammosphere viability by 50%) were extrapolated from dose-response curves (Fig. S11) and are summarised in Table S3. The IC_{50} values for **2a**, **2b**, and **3c** were in the sub-micromolar range, and significantly lower (up to 25-fold) than that reported for salinomycin under the same conditions.[41] The mammosphere potencies of **2a**, **2b**, and **3c** were also better than **1** (up to 6-fold, Fig. S12), cisplatin (up to 12-fold), and dichloro(1,10-phenanthroline)copper(II) (up to 14-fold, Fig. S13). The anti-mammosphere properties observed for **2a**, **2b**, and **3c** are highly desirable in terms of selecting CSC drug candidates for preclinical studies.

Fig. 4 Representative bright-field images (× 10) of HMLER-shEcad mammospheres in the absence and presence of **2a**, **2b**, **3c**, and cisplatin after 5 days incubation.

Insight into the cytotoxic mechanism of action of 3c

To elucidate the possible mechanism of action of the most potent copper(II) complex, **3c** we utilised a mechanism of action predictive functional genetic assay based on RNAi.[42,43] This methodology has been previously applied to shed light on the

mechanism of action of combinations of chemotherapeutics as well as metal-based anticancer agents.[17,44-46] The approach relies on murine cancer cells that are infected with eight green fluorescent protein (GFP)-tagged shRNAs. Each shRNAs confers resistance or sensitivity to a given compound according to its mechanism of action. Thus, the pattern of resistance and sensitivity of the eight shRNAs to a compound of interest can be compared to a reference set of compounds of known mechanism of action. Using this method, we found that the pattern of resistance and sensitivity for **3c** did not relate to any of the compounds in the reference set, which includes all classes of clinical used cytotoxic agents and some recently developed targeted inhibitors. However, when comparing **3c** to cytotoxic agents that are not part of the reference set, the two most similar compounds were dichloro(1,10-phenanthroline)copper(II) and a rhenium(V)-oxo complex previously characterized as a ROS-producing, necroptotosis-inducing agent (Fig. 5).[18,45] By comparing the relative Euclidian distances between **3c**, its closest compounds, and the relationship between and within categories of the reference set, the likelihood that **3c** is related to compounds with unknown mechanisms (within our database) can be determined. The average of the absolute sum of the Euclidian distances from **3c** to dichloro(1,10-phenanthroline)copper(II) and the rhenium(V)-oxo complex are 1.62 and 2.06, respectively. However, the intra-category and inter-category distances of the reference set are 0.99 ± 0.38 and 2.69 ± 0.44, respectively. Thus, the intermediate degree of these similarities is suggestive of related, yet distinct, mechanisms of action (Table S4-5). Interestingly, the Euclidian distance of **3c** from **1** was 2.94 (Table S6), suggesting that **3c** and **1** exhibit similar but distinct mechanisms of action (Fig. S14).

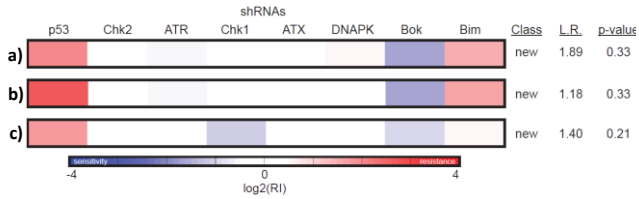

Fig. 5 RNAi signatures derived from the treatment of Eμ-Mycp$^{19arf-/-}$ lymphoma cells with a) **3c**, b) dichloro(1,10-phenanthroline)copper(II), and c) the necroptosis-inducing rhenium(V)-oxo complex at the LD80−90 concentration for each compound.

Intracellular reactive oxygen species (ROS) production by 3c

Given the related mechanism of cytotoxicity of **3c** and known ROS-inducing metal complexes (according to the RNAi assay prediction), we investigated the ability of **3c** to generate ROS in CSC-enriched HMLER-shEcad cells using 6-carboxy-2',7'-dichlorodihydrofluorescein diacetate (DCFH-DA), a fluorescence-based ROS indicator. HMLER-shEcad cells incubated with **3c** (0.5 μM for 6, 12, and 48 h) displayed significantly higher levels of ROS (p < 0.05) compared to untreated cells (Fig. S15-17). A similar enhancement in ROS levels was observed for H_2O_2-treatment (6 μM for 6, 12, and 48 h) (Fig. S15-17). Co-incubation with *N*-acetylcysteine (1.5 mM for 6, 12, and 48 h, a ROS scavenger) reduced **3c**- and H_2O_2-mediated ROS generation (Fig. S15-17). Intracellular generation of ROS can activate stress-activated protein kinase (SAPK)/Jun amino-terminal kinase (JNK) and p38 MAP kinase (MAPK) pathways.[47] Immunoblotting studies showed that HMLER-shEcad cells treated with **3c** (0.25-0.5 μM for 72 h) displayed increased expression of phosphorylated p38 MAPK and SAPK/JNK, and their downstream targets, phosphorylated MAP kinase-activated protein kinase 2 (MAPKAPK-2) and c-Jun (Fig. S18). The activation of SAPK/JNK and p38/MAPK pathways can trigger apoptosis.[48] HMLER-shEcad cells dosed with **3c** (0.25-0.5 μM for 72 h) expressed noticeably higher levels of cleaved caspase-3 and -7 compared to untreated cells, indicative caspase-dependent apoptosis (Fig. S18). Taken together, the data shows that **3c** is able to enhance intracellular ROS levels, activate SAPK/JNK and p38/MAPK pathways, and induce apoptotic cell death. The potency of **3c** towards HMLER-shEcad mammospheres grown in the presence of *N*-acetylcysteine (1.5 mM) decreased significantly (p < 0.05) (Fig. S19 and Table S7). Under these conditions, the ability of **3c** (at the IC_{20} value after 5 days incubation) to reduce the number and size of mammospheres formed was also markedly attenuated (Fig. S20-21). This indicates that the CSC targeting potential of **3c** is, in part, related to its ability to induce ROS.

COX-2 inhibition contributes to 3c-mediated CSC death

COX-2 modulates cell proliferation and apoptosis in solid tumours including breast cancers.[49] COX-2 is also implicated in CSC proliferation and dissemination.[21,50] The COX-2 inhibitory properties of **3c** and indomethacin (positive control) were investigated using an enzyme immunoassay (EIA). COX-2 dosed with **3c** (0.05-50 μM, 37 °C) displayed a marked decrease in activity (conversion of arachidonic acid to PG) compared to untreated control samples with 100% COX-2 activity (Fig. S22). Indomethacin (0.05-50 μM, 37 °C) inhibited COX-2 activity to a similar extent to **3c** (the fact that **3c** contains two indomethacin groups per compound was taken into account in). Collectively the results show that despite the attachment of indomethacin to copper in **3c**, its COX-2 inhibitory effect is retained. Notably, the COX-2 inhibitory effect of **3c** was markedly better than that previously observed for **1**.[18] In order to determine if the cellular mechanism of action of **3c** involves COX-2 downregulation, immunoblotting (Fig. S23) and flow cytometric (Fig. S24A) studies were performed. HMLER-shEcad cells pre-treated with lipopolysaccharide (LPS) (2.5 μM for 24 h), to increase basal COX-2 levels, and treated with **3c** (0.25-0.5 μM for 48 h) or indomethacin (20 μM for 48 h) exhibited a marked decrease in COX-2 expression suggesting that the cytotoxic effect of **3c** may involve COX-2 downregulation. Cisplatin (5 μM) and dichloro(1,10-phenanthroline)copper(II) (8 μM) did noticeably alter COX-2 expression (Fig. S24B). To determine if **3c** evokes COX-2-dependent CSC death, cytotoxicity studies were performed with HMLER-shEcad cells in the presence and absence of prostaglandin E2 (PGE2) (20 μM, 72 h), the product of COX-2-mediated arachidonic acid metabolism. The potency of **3c** towards HMLER-shEcad cells decreased in the presence of PGE2 (2-fold, p < 0.05) (Fig. S25), suggesting that **3c** induces COX-2-dependent CSC death. Additional studies showed that the potency of **3c** towards HMLER-shEcad

mammospheres grown in the presence of LPS (2.5 µM), and PGE2 (20 µM) decreased significantly ($p < 0.05$) (Fig. S19 and Table S7). Under these conditions, the ability of **3c** (at the IC_{20} value after 5 days incubation) to inhibit mammospheres formation was also markedly attenuated (Fig. S20-21). Therefore the ability of **3c** to inhibit COX-2 contributes to its CSC targeting potential.

PEG-PLGA nanoparticle encapsulation of 3c

Biodegradable PEG-PLGA copolymers are amphiphilic, and thus self-assemble in aqueous conditions to form spherical nanoparticles with a hydrophilic PEG outer shell and a hydrophobic PLGA core.[51] The lipophilic copper complex, **3c** (Log P = 1.01) was encapsulated into the hydrophobic core of PEG-PLGA (5000:30000 Da, 1:1 LA:GA) nanoparticles using the nanoprecipitation method (Fig. 6A). Nanoparticles (**3c NP$^{2.5\text{-}50}$**) were prepared using a range of feeds (2.5-50%), where feed refers to the percentage (w/w) of **3c** to polymer. The loading and encapsulation efficiency of **3c** was determined for each formulation by measuring the copper content of the nanoparticles using ICP-MS (after degradation with nitric acid). The change in loading and encapsulation efficiency as function of feed is depicted in Fig. 6B. Maximum encapsulation (where encapsulation efficiency = 1.4% and loading efficiency = 0.07%) was achieved at 5% feed (**3c NP^5**). Characterisation of **3c NP^5** by dynamic light scattering (DLS) showed that the nanoparticle diameter was 145 ± 10 nm, and the polydispersity was 0.218 ± 0.041 (Fig. S26). The nanoparticle size is consistent with previously reported metal complex-polymer formulations.[24,31,52] Due to the PEG outer shell, **3c NP^5** is negatively charged (zeta-potential = −17.5 mV, Fig. S27). The nanoparticle formulation, **3c NP^5** is stable under physiologically relevant conditions (PBS, pH 7.4 with 10% FBS, at 37 °C) over the course of 72 h (Fig. S28), and is able to release an appreciable amount of the payload (**3c**) under similar conditions (PBS, pH 7.4 at 37 °C over 72 h) (Fig. 6C).

Breast CSC uptake, potency, and mechanism of action of the nanoparticle formulation, 3c NP^5

To determine if the nanoparticle construct, **3c NP^5** can enter CSCs, cellular uptake studies were performed. HMLER-shEcad cells were incubated with **3c NP^5** (0.5 µM for 4 h) at 37 °C, and the intracellular copper content was measured by ICP-MS. The nanoparticle formulation, **3c NP^5** was readily taken up by cells under these conditions (174.3 ± 1.3 ppb of Cu/ million cells). The intracellular copper concentration was in fact 10-fold higher than that of the free compound, **3c** under the same conditions (Fig. S29). To determine if uptake was temperature dependent (and thereby active or passive), a similar experiment was conducted at 4 °C (Fig. S29). HMLER-shEcad cells incubated with **3c NP^5** (0.5 µM for 4 h) at 4 °C, displayed a 71% decrease in copper uptake, indicative of active uptake. Polymeric nanoparticles, such as PEG-PLGA are prone to undergo energy- and temperature-dependent endocytosis.[53] To discern if **3c NP^5** undergoes endocytosis, HMLER-shEcad cells were incubated (for 12 h) with endocytosis inhibitors, namely ammonium chloride (50 mM for 2 h) and chloroquine (100 µM for 2 h) prior to treatment with **3c NP^5** (0.5 µM for 12 h) and determination of the intracellular copper levels. Under these conditions, a statistically significant ($p < 0.01$) decrease in uptake was observed (Fig. S30), suggesting that **3c NP^5** enters CSCs via an endocytic pathway. Entities taken up by endocytosis are internalised into endosomes which are acidic. Therefore we investigated the ability of **3c NP^5** to release its payload, **3c**, under acidic conditions (sodium acetate buffer, pH 5.2 at 37 °C over 72 h). The nanoparticle formulation, **3c NP^5** readily releases its payload under these conditions (Fig. 6C), implying that it is capable of releasing **3c** in cells, upon endocytic uptake.

To determine if **3c NP^5** can recapitulate the breast CSC potency and selectivity of the payload, **3c**, cytotoxicity studies were conducted with HMLER and HMLER-shEcad cells. The nanoparticle formulation, **3c NP^5** exhibited sub-micromolar IC_{50} values towards both cell lines (IC_{50} = 0.91 ± 0.02 µM for HMLER cells and IC_{50} = 0.22 ± 0.03 µM for HMLER-shEcad cells, Fig. 6D). Notably, **3c NP^5** was less toxic towards HMLER cells than free **3c** ($p < 0.05$, 2-fold). This is expected, as polymeric nanoparticles are well known to reduce the toxicities of incorporated compounds.[54] Similarly to the payload, **3c NP^5** displayed CSC-selective potency (IC_{50} value for HMLER cells was 4-fold higher than that for HMLER-shEcad cells), which suggests that the mechanism of cytotoxicity of **3c NP^5** and **3c** may be related. The payload, **3c** was found to induce its cytotoxic effect by generating intracellular ROS and inhibiting COX-2 activity (*supra vide*). To decipher if the nanoparticle formulation, **3c NP^5** is able to retain the mechanism action of the payload, further studies were performed. HMLER-shEcad cells incubated with **3c NP^5** (0.5 µM for 48 h) displayed significantly higher levels of ROS ($p < 0.05$) compared to untreated cells (Fig. S31). This shows that **3c NP^5** is able to generate intracellular ROS, like the payload (free **3c**), albeit to a lesser extent. HMLER-shEcad cells pre-treated with LPS (2.5 µM for 24 h) and dosed with **3c NP^5** (0.5-1 µM for 72 h) displayed a drastic decrease in COX-2 levels as evidenced by immunoblotting (Fig. S23) and flow

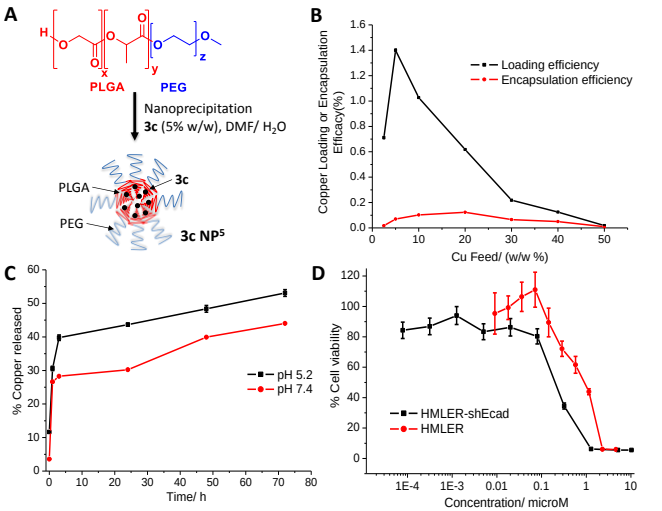

Fig. 6 A) Schematic representation of the preparation of **3c NP^5** using the nanoprecipitation method. B) The effect of feed variation on loading and encapsulation efficiency of **3c** incorporated into PEG-PLGA nanoparticles. C) The amount of copper released from **3c NP^5** upon incubation in PBS (pH 7.4) or sodium acetate buffer (pH 5.2) over the course of 72 h at 37 °C. D) Representative dose-response curves for the treatment of HMLER-shEcad and HMLER cells with **3c NP^5** after 72 h incubation.

cytometric studies (Fig. S24A). This is comparable to the COX-2 downregulation induced by the payload. Collectively, this shows that encapsulation of **3c** by PEG-PLGA copolymers does not alter its cellular properties, which augers well for future *in vivo* development.

Conclusions

In summary we report the synthesis and characterisation of six novel copper(II)-phenanthroline complexes bearing NSAIDs (naproxen, tolfenamic acid, and indomethacin) and their anti-CSC properties *in vitro*. The copper(II) complexes displayed micromolar or sub-micromolar potency towards breast CSC-enriched HMLER-shEcad cells grown in mono- and three-dimensional cell cultures. The CSC potency of two of the complexes, **2a** and **3c** were significantly higher than that of salinomycin, a breast CSC-specific natural product identified in a 16,000 compound screen,[39] and **1**, a related copper(II)-phenanthroline complex recently reported by our group.[18] The same complexes also displayed greater mammosphere-potency than that reported for clinically used drugs; cisplatin, paclitaxel, and vinorelbine.[41] Further, **2b** and **3c** displayed selective potency for CSCs over bulk cancer cells (2-fold), albeit this is lower than that exhibited by salinomycin (3-fold). Detailed mechanistic studies suggest that the cytotoxic mechanism of action of the most effective complex, **3c** involves intracellular ROS generation and COX-2 inhibition. Given our results, it is evident that by combining ROS-generating copper(II)-phenanthroline units and COX-2 inhibiting NSAID moieties within a single molecule, libraries of CSC-potent compounds can be prepared. The leading copper(II) complex, **3c** was successfully encapsulated into PEG-PLGA nanoparticles, **3c NP^5**, which were readily taken up by CSCs through an endocytic pathway. Strikingly, CSC uptake of **3c NP^5** was one order of magnitude greater than that of the unencapsulated copper(II) complex, **3c**. Additionally, **3c NP^5** was 4-fold more cytotoxic towards CSCs than bulk cancer cells, which is moderately better than salinomycin (3-fold). The nanoparticle formulation, **3c NP^5** is not only able to recapitulate the CSC-potency and -selectivity of the payload but also evoke a similar cellular response. The latter bodes well for future in vivo development, as one of the drawbacks of nanoparticle encapsulation as a strategy for drug delivery is the potential discrepancy in cellular mechanism of action of the nanoparticle formulation and its payload.[54] Our results show, for the first time, that CSC-potent metal complexes can be encapsulated by polymeric nanoparticles and delivered into CSCs. Naturally the next step will be to study the nanoparticle formulation presented here, in *in vivo* systems.

Acknowledgements

K.S. is supported by an Early Career Fellowship (ECF-2014-178) from the Leverhulme Trust. A.E. received financial support from a King's College London Faculty Graduate School International Studentship. We are grateful to Prof. Robert Weinberg for providing the HMLER and HMLER-shEcad cell lines used in this study. We thankful to Dr. Timothy Johnstone for his insight and suggestions.

Notes and references

1. L. V. Nguyen, R. Vanner, P. Dirks and C. J. Eaves, *Nat. Rev. Cancer*, 2012, **12**, 133-143.
2. J. Kaiser, *Science*, 2015, **347**, 226-229.
3. J. Marx, *Science*, 2007, **317**, 1029-1031.
4. Y. Yu, G. Ramena and R. C. Elble, *Front. Biosci.*, 2012, **4**, 1528-1541.
5. K. Chen, Y.-h. Huang and J.-l. Chen, *Acta. Pharmacol. Sin.*, 2013, **34**, 732-740.
6. X. Ning, J. Shu, Y. Du, Q. Ben and Z. Li, *Cancer Biol. Ther.*, 2013, **14**, 295-303.
7. M. Al-Hajj, M. S. Wicha, A. Benito-Hernandez, S. J. Morrison and M. F. Clarke, *Proc. Natl. Acad. Sci. U.S.A.*, 2003, **100**, 3983-3988.
8. A. Eramo, F. Lotti, G. Sette, E. Pilozzi, M. Biffoni, A. Di Virgilio, C. Conticello, L. Ruco, C. Peschle and R. De Maria, *Cell Death Differ.*, 2008, **15**, 504-514.
9. C. Li, D. G. Heidt, P. Dalerba, C. F. Burant, L. Zhang, V. Adsay, M. Wicha, M. F. Clarke and D. M. Simeone, *Cancer Res.*, 2007, **67**, 1030-1037.
10. M. E. Prince, R. Sivanandan, A. Kaczorowski, G. T. Wolf, M. J. Kaplan, P. Dalerba, I. L. Weissman, M. F. Clarke and L. E. Ailles, *Proc. Natl. Acad. Sci. U.S.A.*, 2007, **104**, 973-978.
11. S. K. Singh, C. Hawkins, I. D. Clarke, J. A. Squire, J. Bayani, T. Hide, R. M. Henkelman, M. D. Cusimano and P. B. Dirks, *Nature*, 2004, **432**, 396-401.
12. M. Janikova and J. Skarda, *Neoplasma*, 2012, **59**, 6-17.
13. H. Korkaya, A. Paulson, E. Charafe-Jauffret, C. Ginestier, M. Brown, J. Dutcher, S. G. Clouthier and M. S. Wicha, *PLoS Biol.*, 2009, **7**, e1000121.
14. N. Takebe, P. J. Harris, R. Q. Warren and S. P. Ivy, *Nature reviews. Clin. Oncol.*, 2011, **8**, 97-106.
15. M. Gonzalez-Bartulos, C. Aceves-Luquero, J. Qualai, O. Cusso, M. A. Martinez, S. Fernandez de Mattos, J. A. Menendez, P. Villalonga, M. Costas, X. Ribas and A. Massaguer, *PloS One*, 2015, **10**, e0137800.
16. C. T. Lum, A. S. Wong, M. C. Lin, C. M. Che and R. W. Sun, *Chem. Commun.* , 2013, **49**, 4364-4366.
17. K. Suntharalingam, W. Lin, T. C. Johnstone, P. M. Bruno, Y. R. Zheng, M. T. Hemann and S. J. Lippard, *J. Am. Chem. Soc.*, 2014, **136**, 14413-14416.
18. J. N. Boodram, I. J. McGregor, P. M. Bruno, P. B. Cressey, M. T. Hemann and K. Suntharalingam, *Angew. Chem. Int. Ed.*, 2016, **55**, 2845-2850.
19. M. Diehn, R. W. Cho, N. A. Lobo, T. Kalisky, M. J. Dorie, A. N. Kulp, D. Qian, J. S. Lam, L. E. Ailles, M. Wong, B. Joshua, M. J. Kaplan, I. Wapnir, F. M. Dirbas, G. Somlo, C. Garberoglio, B. Paz, J. Shen, S. K. Lau, S. R. Quake, J. M. Brown, I. L. Weissman and M. F. Clarke, *Nature*, 2009, **458**, 780-783.
20. X. Shi, Y. Zhang, J. Zheng and J. Pan, *Antioxid. Redox Signal.*, 2012, **16**, 1215-1228.
21. B. Singh, J. A. Berry, A. Shoher, V. Ramakrishnan and A. Lucci, *Int. J. Oncol.*, 2005, **26**, 1393-1399.
22. B. Singh, K. R. Cook, L. Vincent, C. S. Hall, C. Martin and A. Lucci, *J. Surg. Res.*, 2011, **168**, e39-49.

23. O. C. Farokhzad and R. Langer, *ACS Nano*, 2009, **3**, 16-20.
24. N. P. Barry and P. J. Sadler, *ACS Nano*, 2013, **7**, 5654-5659.
25. R. A. Petros and J. M. DeSimone, *Nat. Rev. Drug Discov.*, 2010, **9**, 615-627.
26. E. Blanco, H. Shen and M. Ferrari, *Nat. Biotechnol.*, 2015, **33**, 941-951.
27. K. Greish, *Methods Mol. Biol.*, 2010, **624**, 25-37.
28. F. Alexis, E. M. Pridgen, R. Langer and O. C. Farokhzad, *Handb. Exp. Pharmacol.*, 2010, DOI: 10.1007/978-3-642-00477-3_2, 55-86.
29. R. Wang, P. S. Billone and W. M. Mullett, *J. Nanomater.*, 2013, **2013**, 12.
30. A. Kumari, S. K. Yadav and S. C. Yadav, *Colloids Surf., B*, 2010, **75**, 1-18.
31. T. C. Johnstone, K. Suntharalingam and S. J. Lippard, *Chem. Rev.*, 2016, **116**, 3436-3486.
32. N. Margiotta, S. Savino, N. Denora, C. Marzano, V. Laquintana, A. Cutrignelli, J. D. Hoeschele, V. Gandin and G. Natile, *Dalton Trans.*, 2016, DOI: 10.1039/c6dt00763e.
33. H. S. Oberoi, N. V. Nukolova, A. V. Kabanov and T. K. Bronich, *Adv. Drug Deliv. Rev.*, 2013, **65**, 1667-1685.
34. X. Wang and Z. Guo, *Chem. Soc. Rev.*, 2013, **42**, 202-224.
35. I. S. Hong, G. B. Jang, H. Y. Lee and J. S. Nam, *Int. J. Nanomedicine*, 2015, **10**, 251-260.
36. W. Rao, H. Wang, J. Han, S. Zhao, J. Dumbleton, P. Agarwal, W. Zhang, G. Zhao, J. Yu, D. L. Zynger, X. Lu and X. He, *ACS Nano*, 2015, **9**, 5725-5740.
37. D. Wang, J. Huang, X. Wang, Y. Yu, H. Zhang, Y. Chen, J. Liu, Z. Sun, H. Zou, D. Sun, G. Zhou, G. Zhang, Y. Lu and Y. Zhong, *Biomaterials*, 2013, **34**, 7662-7673.
38. H. J. Yao, Y. G. Zhang, L. Sun and Y. Liu, *Biomaterials*, 2014, **35**, 9208-9223.
39. P. B. Gupta, T. T. Onder, G. Jiang, K. Tao, C. Kuperwasser, R. A. Weinberg and E. S. Lander, *Cell*, 2009, **138**, 645-659.
40. G. Dontu, W. M. Abdallah, J. M. Foley, K. W. Jackson, M. F. Clarke, M. J. Kawamura and M. S. Wicha, *Genes Dev.*, 2003, **17**, 1253-1270.
41. P. Cressey, A. Eskandari, P. Bruno, C. Lu, M. Hemann and K. Suntharalingam, *ChemBioChem*, DOI: 10.1002/cbic.201600368.
42. H. Jiang, J. R. Pritchard, R. T. Williams, D. A. Lauffenburger and M. T. Hemann, *Nat. Chem. Biol.*, 2011, **7**, 92-100.
43. J. R. Pritchard, P. M. Bruno, M. T. Hemann and D. A. Lauffenburger, *Mol. Biosyst.*, 2013, **9**, 1604-1619.
44. J. R. Pritchard, P. M. Bruno, L. A. Gilbert, K. L. Capron, D. A. Lauffenburger and M. T. Hemann, *Proc. Natl. Acad. Sci. U.S.A.*, 2013, **110**, E170-179.
45. K. Suntharalingam, S. G. Awuah, P. M. Bruno, T. C. Johnstone, F. Wang, W. Lin, Y. R. Zheng, J. E. Page, M. T. Hemann and S. J. Lippard, *J. Am. Chem. Soc.*, 2015, **137**, 2967-2974.
46. K. Suntharalingam, T. C. Johnstone, P. M. Bruno, W. Lin, M. T. Hemann and S. J. Lippard, *J. Am. Chem. Soc.*, 2013, **135**, 14060-14063.
47. J. A. McCubrey, M. M. Lahair and R. A. Franklin, *Antioxid. Redox Signal.*, 2006, **8**, 1775-1789.
48. M. R. Junttila, S. P. Li and J. Westermarck, *FASEB J.*, 2008, **22**, 954-965.
49. C. Sobolewski, C. Cerella, M. Dicato, L. Ghibelli and M. Diederich, *Int. J. Biochem. Cell Biol.*, 2010, **2010**.
50. C. Bocca, M. Ievolella, R. Autelli, M. Motta, L. Mosso, B. Torchio, F. Bozzo, S. Cannito, C. Paternostro, S. Colombatto, M. Parola and A. Miglietta, *Expert Opin. Ther. Targets*, 2014, **18**, 121-135.
51. E. Locatelli and M. Comes Franchini, *J. Nanopart. Res.*, 2012, **14**, 1-17.
52. M. A. Miller, Y. R. Zheng, S. Gadde, C. Pfirschke, H. Zope, C. Engblom, R. H. Kohler, Y. Iwamoto, K. S. Yang, B. Askevold, N. Kolishetti, M. Pittet, S. J. Lippard, O. C. Farokhzad and R. Weissleder, *Nat. Commun.*, 2015, **6**, 8692.
53. G. Sahay, D. Y. Alakhova and A. V. Kabanov, *J. Control. Release*, 2010, **145**, 182-195.
54. W. H. De Jong and P. J. Borm, *Int. J. Nanomedicine*, 2008, **3**, 133-149.